Influence of engine operating variable on combustion to reduce exhaust emissions using various biodiesels blend

M. A. Wakil[1a], H.H. Masjuki[2a], M.A. Kalam[a], Y. H. Teoh[a], H. G. How[a], S. Imtenan[a]

[a]Center for Energy Sciences, Dept. of Mechanical Engineering, University of Malaya, Kuala Lumpur, 50603, Malaysia.

[2]

Abstract

This study focuses mainly on the behavior of biodiesel operated under various operating conditions. The experiment is conducted with B20 of three potential biodiesel sources namely, rice bran, Moringa and sesame oil. A significant outcome is observed from the test results which shows that brake thermal efficiency of biodiesel blend is about 3.4% lower at constant speed running condition than constant torque operating condition. Similarly, about 6.5% lower exhaust gas temperature at constant speed running condition with lower peak pressure are found than at constant torque testing condition. On the subject of emission, it is seen that, testing conditions also have an influential impact on exhaust emission. For instance, at constant speed running condition, the engine produces about 19.5% lower NO and 19% higher HC than at constant torque running condition. A Similar influence is also found in pressure and heat release rate. However, there is a clear variation found in results at different operating conditions. Therefore, it is necessary to test fuel under various operating conditions such as constant torque, constant speed, variable injection timing etc. for the optimal usage of biodiesel.

Keyword: Biodiesel blend, Constant torque, Constant speed, Combustion parameter.

[11] Corresponding Author. Tel: +60163269524; Fax: +6037967531; Email: wakil_01@yahoo.com (M. A. Wakil)
[2] masjuki@um.edu.my (H. H. Masjuki)

1. Introduction

The sustainable production of biofuels is a valuable tool in stemming climate change; boosting local economies, particularly in lesser-developed parts of the world and enhancing energy security for all. Biodiesel is unambiguously found to be a notable option for substituting conventional fuel due to its availability in nature from various renewable biological sources. Besides the valuable advantages, biodiesel has a couple of difficulties to use 100% in an engine such as high viscosity, high density, low volatility and low heating value [1] which lead to problem in pumping, atomization, gumming, injection fouling, piston ring sticking etc. [2]. Consequently, biodiesel blending (biodiesel and diesel) brings a new topic in research arena[3-5].

Among the available sources of biodiesel, a very few are used commercially in different countries. For instance, canola and soybean are used in USA, palm oil in Malaysia, rapeseed oil in Europe etc. [1, 6] However, numerous studies have taken place and are still going on various sources namely, jatropha, rice bran, moringa, coconut, corn, mustard, tallow, karanja, neem, pongamia, linseed, rubber seed etc. for finding out the another valuable source for biodiesel. But different studies have shown different results, more clearly, it is seen that the operating parameters provide significant impact on biodiesel when tested in engines. For example, Niemi et al.[7] tested mustard oil at variable injection timing and found lower NO_x than diesel but A. Sanjid et al.[8] found higher NO_x emission when tested under variable speed condition. Saravanan et al.[9] has shown that rice bran biodiesel possesses lower thermal efficiency, better emission characteristics except the marginal increase in NOx. John & Kumar[10] studied on effect of load on the performance and found that rice bran biodiesel resulted higher brake thermal efficiency than diesel. Patel et al.[11] observed the rice bran biodiesel possessed about (40-50%) less HC and significantly lower CO and NOx. R.S. Kumar et al.[12] tested that at constant speed, all the emissions were lower than diesel except NOx. Similarly, Altun et al.[13] found all the emissions of sesame biodiesel were lower than diesel as well as exhaust temperature. Banapurmath et al.[14] investigated at constant speed, all the emissions of sesame methyl ester had a higher value than diesel except NO.

However, regarding the above mentioned study, it is clear that the study on biodiesel testing under one operating condition can hardly provide exact results which will make it possible to use commercially. It is highly essential to conduct tests under various operating conditions for a particular biodiesel, which will enhance to choose the most potential biodiesel for commercial purpose. Moreover, during road load test, an engine always operates at variable operating parameters such as constant speed with variable load or constant load with variable speed.

Based on the fact, this study is categorized as the investigation of the detailed performance parameters and emission gases under two operating conditions such as constant torque with variable speed and constant speed with variable load. Finally, analysis of in-cylinder combustion such as ignition delay, pressure rise rate, heat release rate and fuel mass burning fraction of the three biodiesel blend in CI engine.

2. Material and methods

2.1 Measurement of physicochemical properties of crude oil and their biodiesel

According to ASTM the physicochemical properties of crude oils and their biodiesel were tested. Chemical properties were tested through chemical testing service. Cetane number (CN), Iodine number (IV) and saponification value (SV) were calculated by using the following equations.

$$CN = 46.3 + \left(\frac{5458}{SV}\right) - (0.225 \times IV) \quad (1)$$

$$SV = \sum \frac{(560.A_i)}{M_{wi}} \quad (2)$$

$$IV = \sum \frac{(254.A_i.D)}{M_{wi}} \quad (3)$$

Where, A_i = the percentage of each fatty acid component;

D = the number of double bond;

M_{wi} = the molecular mass of each component.

2.2 Test fuel and operating condition

In this study, one blend namely B20 (biodiesel 20% vol + diesel 80% vol) of the three feedstock such as Rice bran, Moringa oleifera and Sesame oil were prepared and tested. The experiment was carried out under two operating conditions, Firstly, at constant torque (20 N-m) with varying speed from 1000 rpm to 1800 rpm with a step of 200 rpm and Secondly, at constant speed (1400 rpm) with variable load from 10 N-m to 25 N-m with a step of 5 N-m. Diesel was used as baseline fuel, afterward blended biodiesel such as R20 (Rice bran biodiesel 20% vol.), M20 (Moringa biodiesel 20% vol.) and S20 (Sesame biodiesel 20% vol.) were tested at the same operating condition. During the running condition, the engine ran satisfactorily throughout the entire test. To enhance the accuracy of the study, each test point was repeated twice to derive an average reading.

2.3 Engine test

The experimental investigation was carried out in the Tribology Laboratory of the Department of Mechanical Engineering, University of Malaya, on a single-cylinder, water-cooled, naturally aspirated, direct injection and four-stroke diesel engine. The schematic layout and engine specification is shown in **Figure 1 and Table 1**. In order to provide load to the engine and controlling speed, a ST-7.5 model 7.5 kW A.C. synchronous dynamometer was used. An air flow meter of 2-70 L s^{-1} for intake airflow measurement, A K-type thermocouple for monitoring exhaust gas temperature, a positive displacement gear wheel flow meter (model: DOM-A05H) for fuel flow rate were used. All the necessary sensors were fitted with test system for combustion analysis. A Kistler6125B type pressure sensor was used for in-cylinder gas pressure measurement. To eliminate the cycle to cycle variation in each test, an average data was calculated from 100 consecutive combustion cycles of pressure data. To reduce noise effects, smooths data using SPAN as the number of points used to compute each element was applied to the sampled cylinder pressure data. A Bosch BEA-350 exhaust gas analyzer was used for engine emissions analysis of HC, CO, CO_2 and NO. Bosch RTM 430 smoke opacity meter was used to measure the smoke opacity. Specification of emission analyzer is given in **Table 2**. The same method was applied for all blends.

Figure 1: Schematic diagram of engine test bed

Table 1: Specification of the engine

Table 2: Specification of emission analyzer

2.4 Analysis of cylinder pressure data and heat release

In order to obtain quantitative information on the progress of combustion, the data of cylinder pressure versus crank angle is significant [15]. For a proper analysis of heat release rate the average value of 100 cycles was considered, as average of N measurements is more reliable estimator for the average pressure at that crank angle than any individual cycle measurement. The heat release rate, $\frac{dQ}{d\theta}$ per degree crank angle derived from the first law of thermodynamics and can be calculated by equation- 4.

$$\frac{dQ}{d\theta} = \frac{\lambda}{\lambda - 1} P \frac{dV}{d\theta} + \frac{1}{\lambda - 1} V \frac{dP}{d\theta} \text{.............................}(4)$$

Where, $\frac{dQ}{d\theta} =$ rate of heat release (J/°CA), V = instantaneous cylinder volume (m^3), $\theta =$ crank angle (°CA), P = instantaneous cylinder pressure (Pa), $\gamma =$ specific heat ratio which is considered constant at 1.35.

3. Results and discussion

3.1 Characterization of crude oils and their biodiesel

The basic properties of the crude oils and their biodiesel are shown in **Table 3.** It is seen from Table 3 that rice bran biodiesel possesses relatively more density and viscosity than sesame and moringa biodiesel. The cetane number calculated for rice bran biodiesel is found higher (76.1) than sesame (54.3) and moringa (51.3). Oxygen content of all the biodiesel is about 11% with about 12% hydrogen. Flash point of sesame biodiesel is more compared to rice bran and moringa biodiesel.

Table 3. Physicochemical characteristics of crude oils and biodiesel

n.s ≡ not specified; N/D ≡ not determined.
CRBO ≡ Crude rice bran oil
CMOO ≡ Crude Moringa oil
CSO ≡ Crude sesame oil
RME ≡ Rice bran biodiesel
MME ≡ Moringa biodiesel
SME ≡ Sesame biodiesel

3.2 Effect of operating parameters on engine performance, emission and combustion

3.2.1 Brake specific fuel consumption

BSFC analysis is imperative because fuel economy is commonly assessed in terms of distance for transportation vehicles. **Figure 2** shows the variation of BSFC under two operating conditions such as constant torque and constant speed. The average BSFC of all biodiesel blends are found higher about 3.11% than diesel in each operating condition. The reason might be slightly higher density and lower calorific value of biodiesel [16, 17]. For the same volume of fuel injection, the amount of injected biodiesel is higher than that of diesel[18]. A higher required amount and a lower calorific value lead to higher volumetric consumption for the same brake power output [19]. BSFC is in increasing trend as the speed increases, but reversing trend observes when load rises shown in **Figure 2**. Frictional loss is the main cause of higher BSFC because with the increase of speed, frictional loss also increases, but at constant speed with increasing load, the decreasing trend of BSFC is dominated by increasing mechanical efficiency as bmep increases [15]. It is observed that BSFC at constant speed are higher about 4.38% on average than BSFC at constant torque. The average BSFC at constant torque calculated are 295.9, 306.5, 306.86 and 307.29 g /kW-h for Diesel, M20, R20 and S20 respectively. On the other hand, at constant speed the values are 308.89, 317.02, 319.57 and 320.36 g/kW-h for Diesel, M20, R20 and S20 respectively. In terms of brake specific energy consumption, all fuels, including diesel possess higher energy consumption about 4.05% at variable load condition than at variable speed running condition. But all biodiesel possesses slightly higher specific energy consumption about 1-1.5% than diesel. Moreover, it is observed that, M20 provides lower energy consumption followed by R20 and then S20.

Figure 2: Variation in brake specific fuel consumption at variable operating condition

3.2.2 Exhaust temperature

The variation in exhaust temperature with the variation in both engine speed and load for biodiesel blends are shown in **Figure 3**. It is seen that exhaust gas temperature increases for both aforementioned operating conditions. Such phenomena are the result of variations in the relative importance of heat transfer in the cylinder and heat transfer to the exhaust valve and port. The amount of fuel combusted in the combustion chamber within a unit time increases; consequently, the heat energy produced increases as the engine speed increases [20]. It is seen that, with the increase in speed exhaust temperature for both diesel and biodiesel rise to 1-10.92% on average, but such variation at constant speed condition is larger than at variable speed, for instance, 12.38-20.42%. However, all biodiesel exhibit higher exhaust temperatures than diesel, for example, 2.53% at constant torque and 1.05% at constant speed on average. Such differences are due to physical delay because proper atomization is retarded by high density and viscosity [21]. However, on average, exhaust temperature rise at constant torque is more about 6.54% than formed at constant speed condition.

Figure 3: Variation in exhaust gas temperature at variable operating condition

3.2.3 Brake thermal efficiency

Brake thermal efficiency is mostly related to BSFC and calorific value. It is seen from **Figure 4** that brake thermal efficiency (BTE) for biodiesel blends follow the same trend line as diesel. It is found that biodiesel blends possess about 1.42% lower BTE on average than diesel. The relatively higher fuel consumption and lower calorific value of biodiesel are the main cause for such result. It is seen that BTE at low and average speed is higher than at higher speed because at lower speed, minimum heat loss cause lower fuel consumption but at higher speed, frictional loss dominate the situation. On the other hand, when the fuels are tested under constant speed, keeping load variable, it is seen that BTE is improving. At constant speed, when load is increasing the brake power is also improving which in turn increase BTE. It is found that BTE at constant speed is about 3.4% lower than at constant torque operating condition on average.

Figure 4: Variation in brake thermal efficiency at variable operating condition

3.2.4 Ignition delay

Ignition delay, an important phenomenon of combustion, is defined as the time interval between the start of injection and the start of combustion [15]. Both physical and chemical processes take place in the duration of ignition delay, which largely depends on the fuel ignition characteristics (cetane number). The influence of operating conditions on ignition delay is presented in **Figure 5**. Ignition delay or delay period increases linearly when operating speed increases. A change in engine speed changes the temperature/time and pressure/time relationships [15]. The negative impact is found when the fuels are tested under variable load condition. The delay decreases linearly as the load increases. Because with the addition of load, both the residual gas temperature and wall temperature increases, which results high charge temperature at injection. This reduces the delay [15].

Figure 5: Variation in ignition delay at variable operating condition

3.2.5 Peak pressure

Figure 6 shows the effect of testing conditions on combustion peak pressure. It is observed that peak pressure of any fuel is largely depends on heating value and ignition delay. In some cases, it is found that biodiesel possesses a higher peak pressure than diesel because the relatively longer ignition delay of these biodiesel have compensated the negative impact of the lower calorific value. A longer ignition delay accumulates more oil to burn initially, consequently increasing the pressure [22]. However, both operating conditions have an influence on peak pressure. **Figure 6** shows that the peak pressure increases with an escalation in speed, and the variation is maximized at a high speed except at the initial speed. The vital factor effecting such a variation is ignition delay: as speed increases, ignition delay increases [15]. On the other hand, under constant speed, when load is increasing the peak pressure also increases linearly, not as sharp as at constant torque condition. With the rise of load the mean effective pressure rises because of improving mechanical efficiency. For that reason, peak pressure is improving as load increases, though the load has negative impact on ignition delay. It is tested that all the fuels give more peak pressure at constant torque condition than at constant speed running, about 8.8% on average.

Figure 6: Variation in peak pressure at variable operating condition

3.2.6 Pressure rise, heat release rate and mass burnt fraction

Pressure rise rate and heat release rate are significant in combustion analysis because these parameters can help to sufficiently assess the engine performance and the effects of operating conditions on engine performance, as well as to compare the performance of different engines under the same operating conditions [23]. It is observed that the operating conditions have an influence on maximum pressure and heat release developed (**Figure 7**). For instance, on crank angle basis maximum pressure rise at constant torque forms at about 1.875°CA earlier (average data) than at constant speed running condition. But the maximum heat release rate for constant torque condition happen at about 2.5°CA later on average than at constant speed condition. The reason might be the time of residence. At constant torque, as the speed increases the residence time for fuels inside the cylinder decreases. For such reason the proper combustion timing is redeemed by longer crank rotation. At constant torque, the maximum pressure rises at 8.75°CA to 14.75°CA and maximum heat release at 7.125°CA to 13.75°CA. On the other hand, at constant speed, the pressure rise maximizes at 10.75°CA to 16.5°CA and heat release maximizes at 6.875°CA to 7.875°CA. At lower speed/load, the maximum pressure rise for biodiesel blends is few crank angle degree later than diesel. Relatively higher viscosity, lower heating value and lower in cylinder pressure are responsible for such results. Another important finding from the experiment is that, with an increase in speed, the heat release rate is lesser than that at the lower speed. The maximum heat release occurs at the initial speed because of the starting condition of the engine, in which some gases are trapped in the crevice region, thereby increasing heat transfer [15]. In the case of fuel burning, the mass burnt fraction (MBF) curves of all biodiesel follow the same trend as that of diesel, the burning rate of all fuels increase with an increase in speed/load because the burning interval remains constant on the CA basis [15].

Figure 7. A1: At 1000 rpm

Figure 7.B1: At 10 N-m

Figure 7.A2: At 1800 rpm

Figure 7.B2: At 25 N-m

Figure 7: Variation in pressure rise, heat release and mass burning rate at variable operating condition

3.2.7 Exhaust emissions

3.2.7.1 Nitric oxide

The formation of nitrogen oxides largely depends on peak flame temperature, high burning gas temperature, ignition delay, and availability of nitrogen and oxygen [15]. The present study deals with NO (nitric oxide) because it is the principal oxide of nitrogen. From **Figure 8** it is seen that the formation of NO is lower at an average speed than at the initial and final operating speeds. At 1000 rpm, NO is higher because at a lower speed, the residence time of injected fuel is higher which enhance the proper atomization and vaporization of fuels. This leads to the burning of fuels nearer to the peak combustion temperature and pressure[15]. Thus increase NO formation. At a speed of 1800 rpm, combustion is enhanced by advanced injection, which prolong the combustion, and thus NO formation again becomes higher. On the other hand, at low load (**Figure 8**), NO formation is lower because of lower cylinder pressure and temperature [24]. But as the load increases at a certain speed, NO formation is also increasing except at high load. When the load rises, the fuel-air ratio also rises up steadily with the increasing of bmep. The increased quantity of fuel injected per cycle results in an increase amount of charge close to stoichiometric combustion, consequently near to peak pressure and temperature [15]. Thus NO is going higher. But when the load is going higher for maximum, NO formation is going down. The increased amount of fuel injected at high load results rich mixture and lower volumetric efficiency due to high in-cylinder temperature. These two phenomena are responsible to burn fuel initially slower. This is in-turn leads proper atomization and vaporization which cause burning of fuel at the end of combustion with sufficient amount of oxygen which result relatively low peak ignition temperature. Thus NO formation decreases. It is observed that NO formation at constant speed is about 19.5% lower than at constant torque operating condition.

Figure 8: Variation in nitric oxide at variable operating condition

3.2.7.2 Hydrocarbon

Figure 9 shows the variation of hydrocarbon (HC) at different operating conditions. It is observed that, HC formation increases as speed increases. This finding can be attributed to over-fueling as the engine accelerates [15]. The sac volume (the small volume left at the tip of the injector after the needle seats) is filled with fuel, and because of over-fueling, it can hardly mix with air. For that reason, HC formation increases [25]. On the other hand, the HC formation at light load is found higher than higher load due to overleaning. Because at light load the mixture is too lean to stoichiometric ratio, which is one of the vital factors for higher HC[15]. It is found that unburnt hydrocarbon formation at constant speed running condition is about 19% higher than at constant torque operating condition on average. It is also found that, different operating conditions effect on biodiesel's HC formation. For instance, M20 possesses lower HC than R20 and S20 at constant speed running condition, but contrary results found when operated at constant torque.

Figure 9: Variation in unburnt hydrocarbon at variable operating condition

3.2.7.3 Carbon monoxide and smoke opacity

The formations of CO and smoke are shown in **Figure 10.** The data show that the formation of CO is largely depends on operating condition. As seen in the figure, CO of biodiesel blends at constant torque condition is higher than diesel. On the other hand, at constant speed, the formation of CO is lower than diesel on average except S20. With the increase of load, the residual gas temperature and wall temperature are both increases which promote in cylinder temperature. Thus, proper atomization is enhanced which improve complete combustion of biodiesel blends as biodiesel contains about 11% more oxygen than diesel (shown in **Table 3**). It is found that CO formation at initial operating condition is higher than others. Improper combustion due to the idling and entrapment of some fuels in crevice zone is the vital reason of such results [15]. It is examined that CO formation for M20 higher than R20 at variable speed, but when tested at constant speed, it is seen that R20 possesses higher CO formation than M20 especially at high load.

Figure 10: Variation in carbon monoxide at variable operating condition

The smoke form in the exhaust tail pipe is usually visible as black smoke. The composition of smoke highly depends on the type of fuel, engine operating condition and residue of carbon [26]. It is found (**Figure 11**) that at high speed and high load operating condition, all the fuels, including diesel have possessed more smoke than normal operating conditions. Because the sudden acceleration from one speed to another causes over-fueling to ensure balance. This outcome initially results in a rich mixture, which in turn leads to smoke formation. The same results found at high load operating condition.

Figure 11: Variation in smoke opacity at variable operating condition

4. Conclusion

Due to the high demand of eco-friendly fuels for transportation, the search for new source of biodiesel is ongoing. As consensus, this study is carried out through various operating conditions because of the limitation of single operating condition, mentioned above. The findings from the above study have shown that operating parameters have significant impact on both performance, emission and combustion, but the impact is higher on emissions. To conclude, more than one test condition is highly demanding for testing biodiesel, if it is considered for commercial purposes.

Acknowledgement

The authors would like to acknowledge the University of Malaya for financial support through the High Impact Research grant titled: Development of Alternative and Renewable Energy Career (DAREC); grant number UM.C/HIR/MOHE/ENG/60.

Reference

1. A. S. Silitonga, H. H. Masjuki, T. M. I. Mahlia, H. C. Ong, W. T. Chong and M. H. Boosroh, *Renewable and Sustainable Energy Reviews*, 2013, **22**, 346-360.
2. N. Kumar, Varun and S. R. Chauhan, *Renewable and Sustainable Energy Reviews*, 2013, **21**, 633-658.
3. M. I. Arbab, H. H. Masjuki, M. Varman, M. A. Kalam, H. Sajjad and S. Imtenan, *RSC Advances*, 2014, **4**, 37122-37129
4. A. Sanjid, H. H. Masjuki, M. A. Kalam, S. M. A. Rahman, M. J. Abedin and I. M. R. Fattah, *RSC Advances*, 2015, **5**, 13246-13255
5. A. B. Koc and M. Abdullah, *Fuel Processing Technology*, 2014, **118**, 264-269.
6. P. Saxena, S. Jawale and M. H. Joshipura, *Procedia Engineering*, 2013, **51**, 395-402.
7. S. A. Niemi, P. E. Illikainen and V. O. K. Laiho, *SAE International*, 1997, DOI: 10.4271/972724, 17.
8. A. Sanjid, M. A. Kalam, H. H. Masjuki, S. M. A. Rahman and M. J. Abedin, *RSC Advances*, 2014, DOI: DOI: 10.1039/C4RA05085A, 36973-36982
9. S. Saravanan, G. Nagarajan and G. L. Narayana Rao, *Energy for Sustainable Development*, 2009, **13**, 52-55.
10. M. M. John and V. Kumar, *Journal of Basic and Applied Engineering Research*, 2014, **1**, 14-17.
11. S. I. Patel, D. C. Gosai and V. Y. Gajjar, *International Journal of Engineering and Advanced Technology (IJEAT)*, 2013, **2**.
12. R. S. Kumar and R.Manimaran, *International Journal of Science, Engineering and Technology Research (IJSETR)*, 2014, **3**.

13. Ş. Altun, H. Bulut and C. Öner, *Renewable Energy*, 2008, **33**, 1791-1795.

14. N. R. Banapurmath, P. G. Tewari and R. S. Hosmath, *Renewable Energy*, 2008, **33**, 1982-1988.

15. John B. Heywood, *Internal combustion engine fundamentals.* , McGraw-Hill, Inc. , 1988.

16. M. Shahabuddin, A. M. Liaquat, H. H. Masjuki, M. A. Kalam and M. Mofijur, *Renewable and Sustainable Energy Reviews*, 2013, **21**, 623-632.

17. M. Habibullah, H. H. Masjuki, M. A. Kalam, I. M. Rizwanul Fattah, A. M. Ashraful and H. M. Mobarak, *Energy Conversion and Management*, 2014, **87**, 250-257.

18. M. Jindal, P. Rosha, S. K. Mahla and A. Dhir, *RSC Advances*, 2015, **4**.

19. I.M. Rizwanul Fattah, M. A. Kalam, H. H. Masjuki and M. A. Wakil, *RSC Advances*, 2014, DOI: 10.1039/C3RA47954D 17787-17796.

20. H. C. Ong, H. H. Masjuki, T. M. I. Mahlia, A. S. Silitonga, W. T. Chong and K. Y. Leong, *Energy Conversion and Management*, 2014, **81**, 30-40.

21. N. Usta, *Energy Conversion and Management*, 2005, **46**, 2373-2386.

22. Lakshmi Narayana Rao G, Saravanan S, Sampath S and R. K., *Thermal science*.

23. J. Ghojel and D. Honnery, *Applied Thermal Engineering*, 2005, **25**, 2072-2085.

24. E. Öztürk, *Fuel Processing Technology*, 2015, **129**, 183-191.

25. Willard W. Pulkrabek, *Engineering Fundamentals of the Internal Combustion Engine*, Prentice Hall, 2003.

26. Y. H. Teoh, H. H. Masjuki, M. A. Kalam, M. A. Amalinaa and H. G. How, *RSC Advances*, 2014, **4**, 50739-50751.

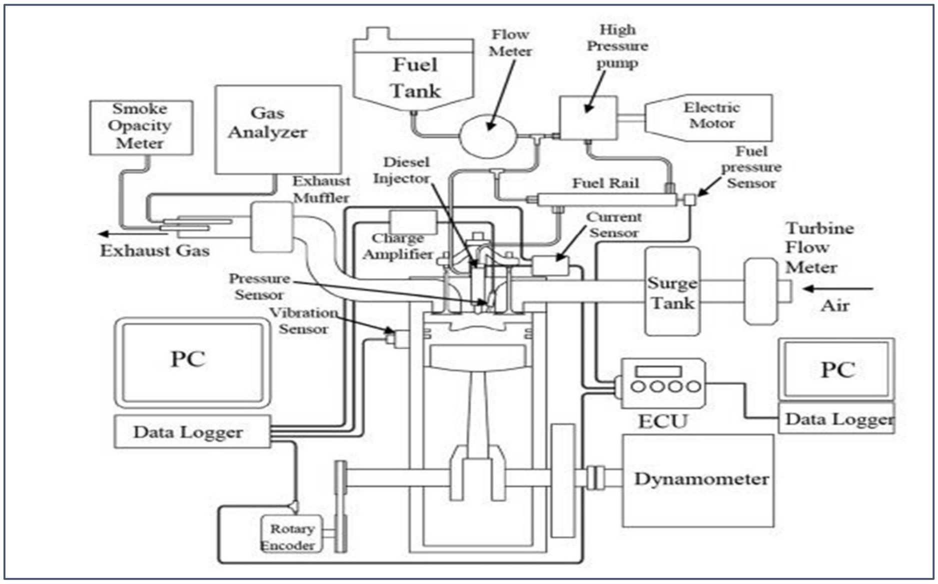

Figure 1: Schematic diagram of engine test bed

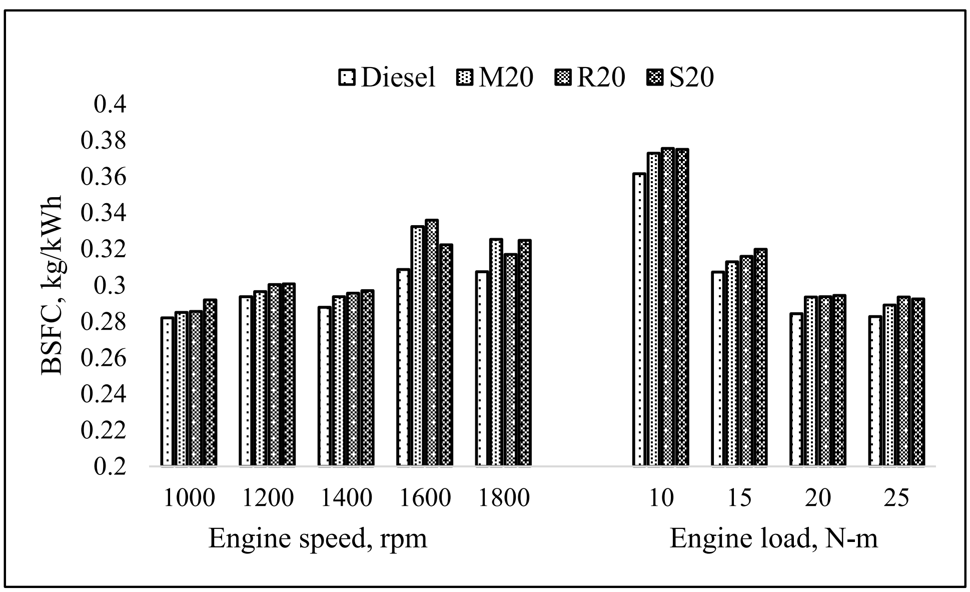

Figure 2: Variation in brake specific fuel consumption at variable operating condition

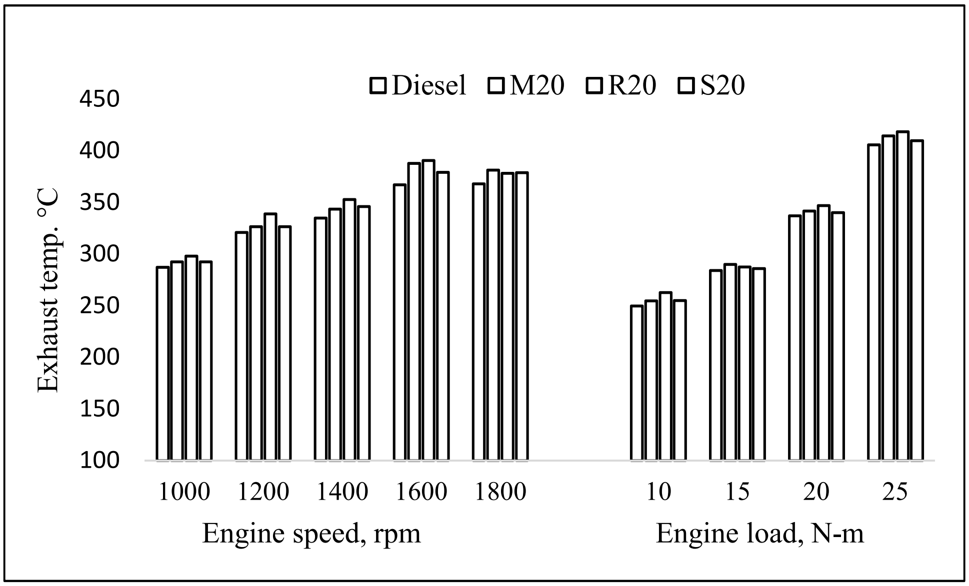

Figure 3: Variation in exhaust gas temperature at variable operating condition

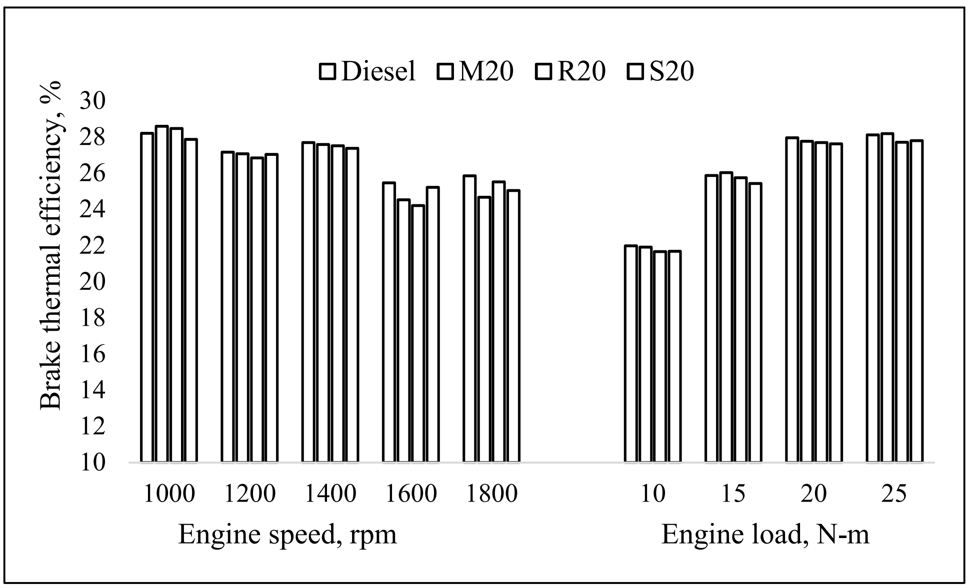

Figure 4: Variation in brake thermal efficiency at variable operating condition

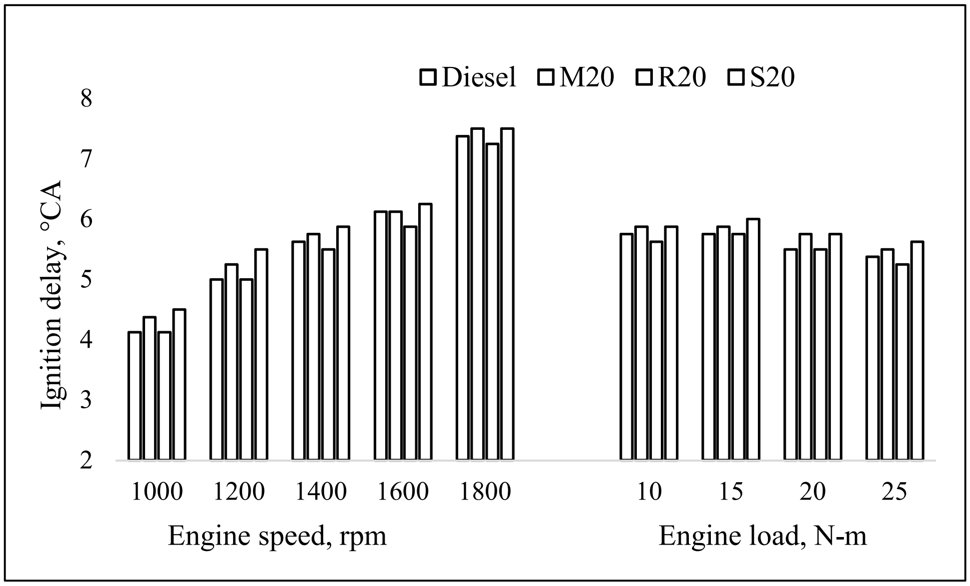

Figure 5: Variation in ignition delay at variable operating condition

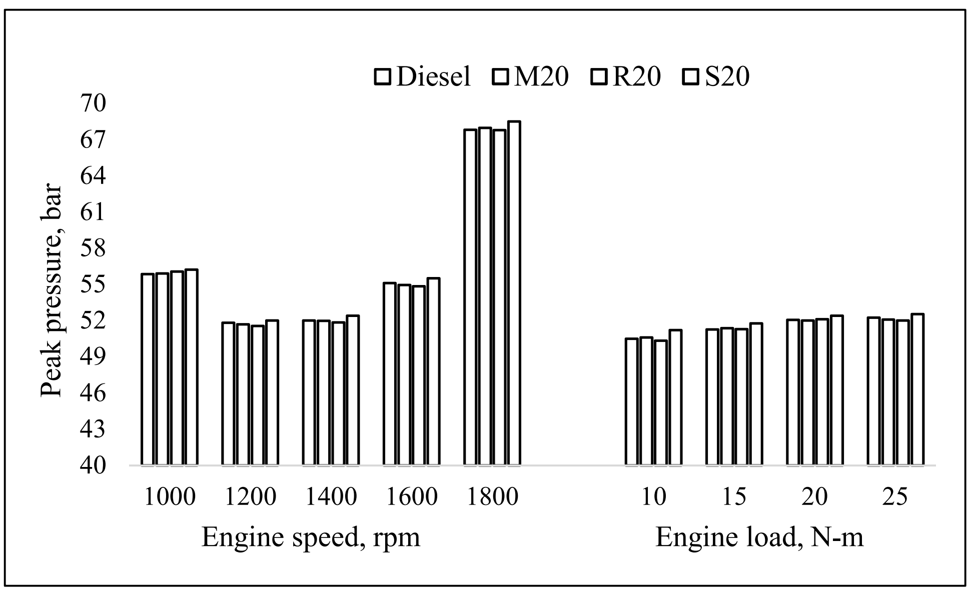

Figure 6: Variation in peak pressure at variable operating condition

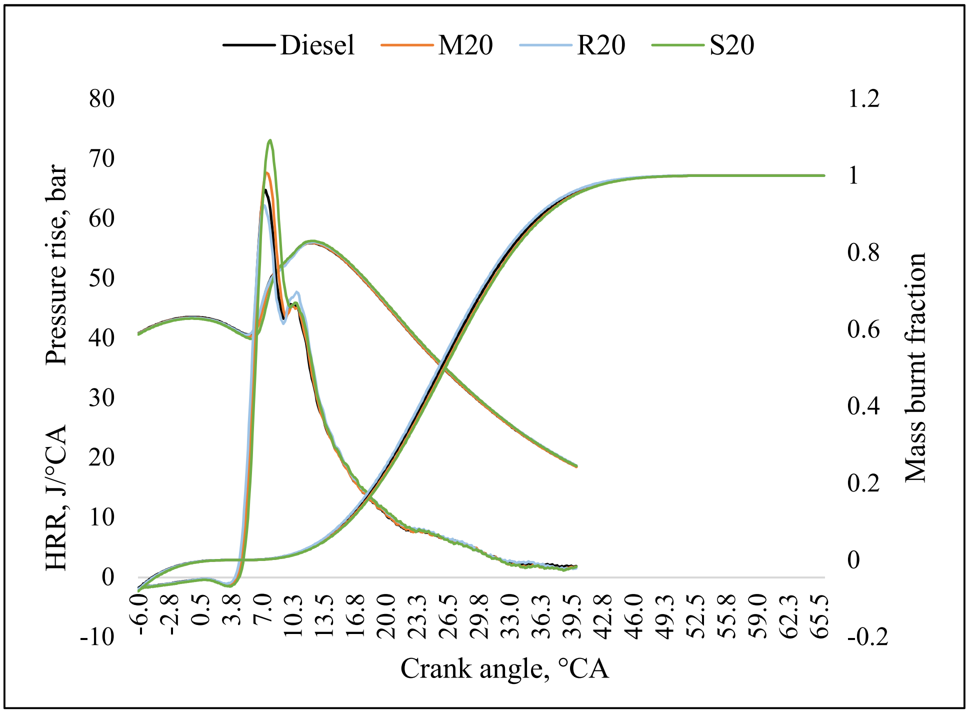

Figure 7. A1: At 1000 rpm

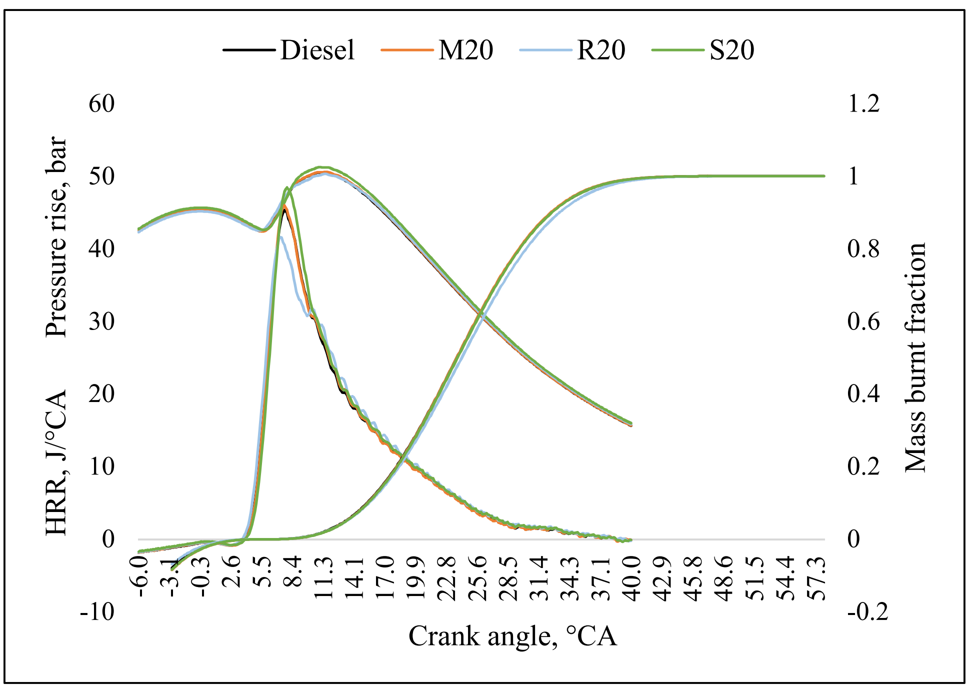

Figure 7.B1: At 10 N-m

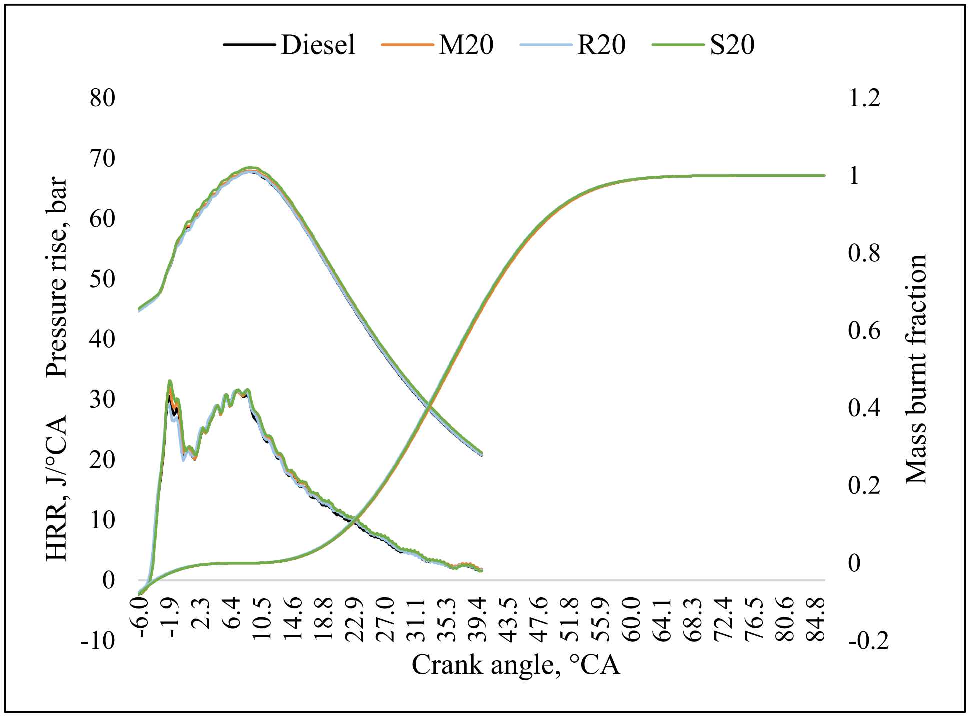

Figure 7.A2: At 1800 rpm

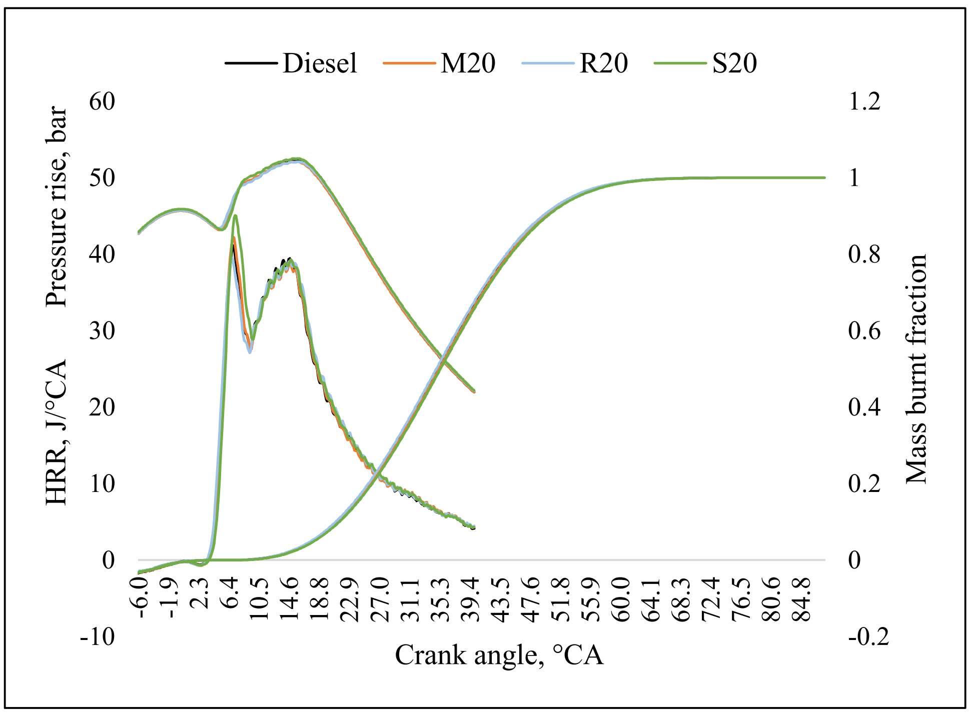

Figure 7.B2: At 25 N-m

Figure 7: Variation in pressure rise, heat release and mass burning rate at variable operating condition

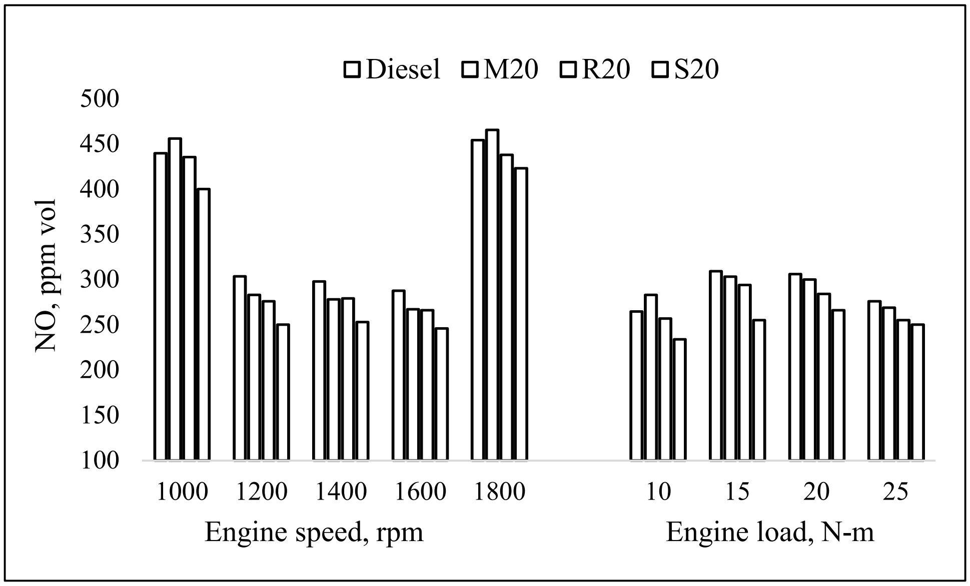

Figure 8: Variation in nitric oxide at variable operating condition

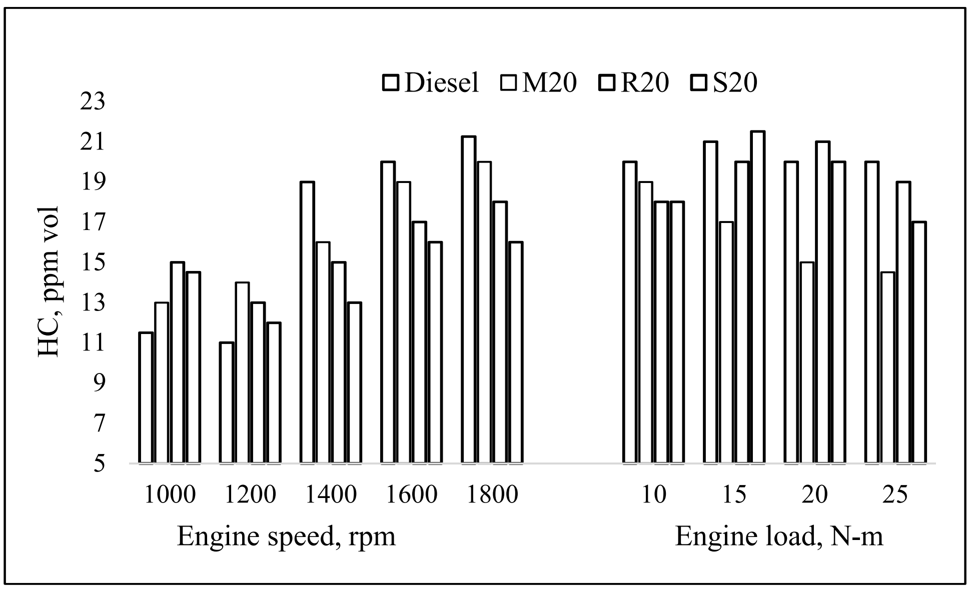

Figure 9: Variation in unburnt hydrocarbon at variable operating condition

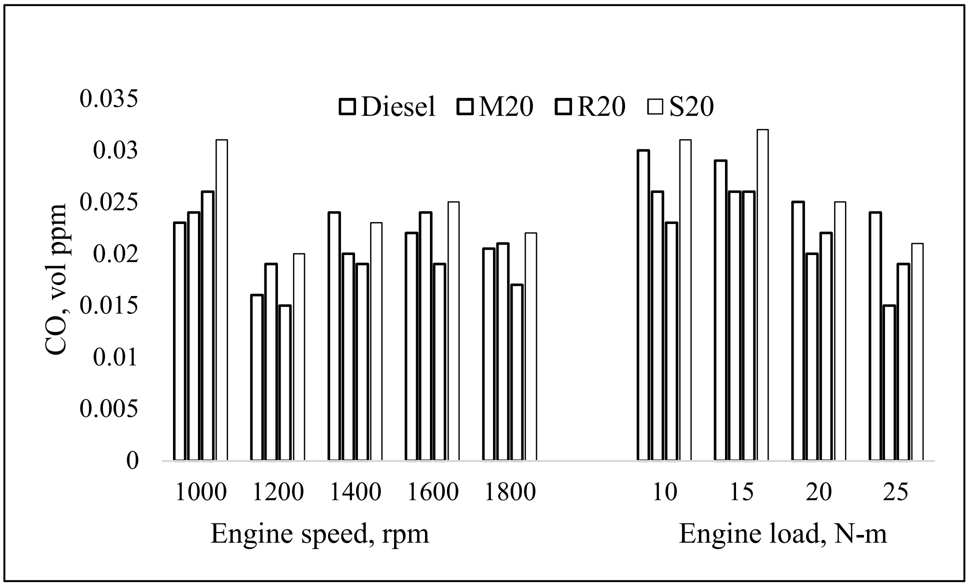

Figure 10: Variation in carbon monoxide at variable operating condition

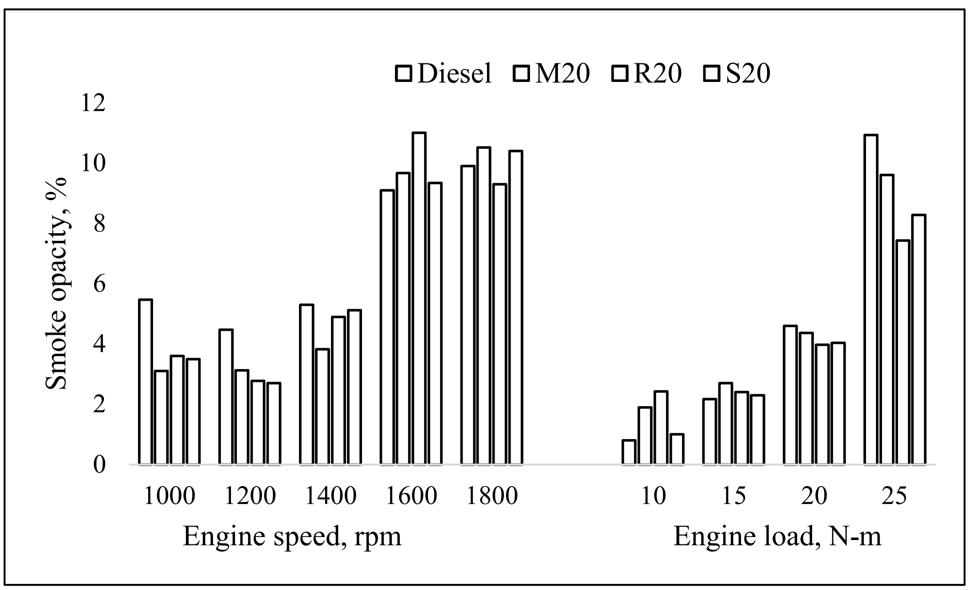

Figure 11: Variation in smoke opacity at variable operating condition

Table 1: Specification of the engine

PARAMETER		UNITS
Displacement	638	cm^3
Bore × Stroke	92 × 96	mm × mm
Compression ratio	17.7 : 1	
Rated power	7.8	kW
Rated speed	2400	rpm
D/H_{BOWL}	2.81	
Combustion chamber	Re-entrant type	
Fuel injection type	Mechanical cam driven injection	
No. of injection holes	4	
Nominal injection nozzle diameter	0.26	mm

Table 2: Specification of emission analyzer

Equipment	Method	Measurement	Upper limit	Accuracy
BOSCH gas analyzer	Non-dispersive infrared	CO	10.00 vol.%	±0.02vol%
	Non-dispersive infrared	HC	9999 ppm	±1 ppm
BOSCH RTM 430	Photodiode receiver	Smoke opacity	100%	± 0.1%
AVL DICOM 4000	Electrochemical	NOx	5000 ppm	±1 ppm

Table 3. Physicochemical characteristics of crude oils and biodiesels

Property	Unit	CRBO	CMOO	CSO	RME	MME	SME	ASTM D6751	EN 14214	Diesel
Kinematic viscosity at 40°c	mm^2/s	52.225	32.004	34.087	5.3657	4.1264	4.3989	1.9-6.0	3.5-5.0	3.1818
Density at 15°c	kg/m^3	924.3	923.4	923.6	886.9	885.8	884.8	n.s	860-900	849.1
Higher heating value	MJ/kg	39.548	39.868	39.386	39.957	39.888	39.996	n.s	n.s	45.315
Flash point	°C	300.5	263.5	280.5	174.5	176.5	208.5	>130	>120	73.5
Cetane number		N/D	N/D	N/D	76.1	51.3	54.3	47 min.	51 min.	N/D
Iodine value		N/D	N/D	N/D	92.88	127.55	108.03			N/D
Saponification value		N/D	N/D	N/D	143.53	161.93	168.93			N/D
Oxygen content	wt%	N/D	N/D	N/D	11	11.9	10.7	11	n.s	0.6
Carbon content	wt%	N/D	N/D	N/D	76.1	75.8	76.5		n.s	84.6
Hydrogen content	wt%	N/D	N/D	N/D	12.9	12.3	12.8	12	n.s	14.8

n.s ≡ not specified; N/D ≡ not determined.
CRBO ≡ Crude rice bran oil
CMOO ≡ Crude Moringa oil
CSO ≡ Crude sesame oil
RME ≡ Rice bran biodiesel
MME ≡ Moringa biodiesel
SME ≡ Sesame biodiesel